Published in final edited form as:
Langmuir. 2010 May 4; 26(9): 6193–6200. doi:10.1021/la1010067.

Light Driven Formation and Rupture of Droplet Bilayers

Sanhita S. Dixit*, **Hanyoup Kim**, **Arseny Vasilyev**, **Aya Eid**, and **Gregory W. Faris**
Molecular Physics Laboratory, SRI International, 333 Ravenswood Avenue, Menlo Park, CA 94025

Abstract

We demonstrate optical manipulation of nanoliter aqueous droplets containing surfactant or lipid molecules and immersed in an organic liquid using near infrared light. The resulting emulsion droplets are manipulated using both the thermocapillary effect and convective fluid motion. Droplet pair-interactions induced in the emulsion upon optical initiation and control provide direct observations of the coalescence steps in intricate detail. Droplet-droplet adhesion (bilayer formation) is observed under several conditions. Selective bilayer rupture is also realized using the same infrared laser. The technique provides a novel approach to study thin film drainage and interface stability in emulsion dynamics. The formation of stable lipid bilayers at the adhesion interface between interacting water droplets can provide an optical platform to build droplet-based lipid bilayer assays. The technique also has relevance for understanding and improving microfluidics applications by devising Petri dish based droplet assays requiring no substrate fabrication.

Introduction

Traditional microfluidics devices rely on the fabrication of intricate circuits to control the direction, flow, and mixing of liquids in narrow channels to mimic laboratory-based experiments in chemistry and biology at the microscale.[1] The possibilities offered are enormous, and much progress has been made over the past decade in utilizing this technology in a wide range of applications. For example, microfluidic platforms have been used to develop assays to measure cellular membrane potential,[2] perform single cell analysis[3-5] and study bacterial chemotaxis.[6] The natural evolution of this technology in the direction of compartmentalization of reagents and reducing their concentrations in biochemical assays steered the research community towards exploring droplet-based microfluidic systems in the form of water-in-oil emulsions as micro-reactors in microfluidic devices.[7-10] The ability to confine biomolecules in picoliter to femtoliter aqueous reservoirs[7] has fuelled the development of droplet-based microfluidic platforms for a range of applications including but not limited to enzymatic assays,[11, 12] polymerase chain reactions[13-15] and protein expression in single cells.[16] Typically, drop motion in microfluidic systems based on channels is enabled through the use of pumps[17] using controlled flow rates. Recently, interest has increased in developing methods to directly maneuver droplets in these devices to avoid the use of external flows. The ability to control droplet motion is an important factor in the development of future applications with this technology to mix, sort and split drops.[18] Several approaches have been demonstrated using thermoelectric manipulation, vibration actuation, dielectrophoresis, electrowetting and magnetic forces.[19-23] A direct impact of this technology has been in the application of droplet-based microfluidic techniques to study interesting phenomena in the dynamics of emulsion stability and droplet coalescence.[24-28] For example, Baret *et al.*[29] use microfluidics devices to investigate the kinetic aspects of emulsion stabilization by surfactants. Numerous experiments

* Corresponding author. Tel: +1 650 859 4614, sanhita.dixit@sri.com.

Supporting Information Paragraph: An online video demonstrating the formation of an adhesive droplet pair for images shown in Figure 4 is available online. A second video details the sequence of events in the formation of lipid bilayers in Figure 6.

from Dr. Jérome Bibette's group have investigated the coalescence of emulsion drops using decompression[25] and electric fields.[30]

The use of optical forces has been recently shown to be an alternate powerful approach for developing droplet-based microfluidic platforms[10, 31-35] in systems where aqueous droplets are immersed in an organic phase. Thermal methods for optically-assisted drop manipulation can be based on: (i) light absorption in the droplet (or organic phase) through a molecular vibrational absorption resonance in the water (organic) phase or (ii) via absorption by dye molecules added to the water (or organic) medium. This absorption of light energy increases the temperature of the water drop (or organic phase) in the vicinity of the laser spot. This local heating changes the water-organic interfacial tension and produces recirculation flows in the droplet and the surrounding organic phase. The resulting migration of the droplet in response to these flows is defined as the thermocapillary (thermal Marangoni) effect.[36-39]

In the classical thermocapillary effect first reported by Young *et al.*[40] air bubbles in a vertical liquid column moved toward hotter regions against buoyancy. In experiments in our laboratory, [10] we observed an opposite effect. Specifically, we used a laser (e.g., at 1550 nm, a wavelength that is strongly absorbed by water) to heat one edge of a water drop immersed in decanol (in a Petri dish). We observed that the water drop migrated away from the laser—opposite to the temperature gradient and in a direction inconsistent with conventional thermocapillary migration.[41, 42] This observation can be explained by the anomalous temperature dependence of the water-decanol interfacial tension (γ): the interfacial tension increases with temperature, reaching a maximum around 80°C before a reverse trend occurs.[43] Thus, an increase in the interfacial tension results in a Marangoni stress that pulls the interface (black arrows in Figure 1a) towards the high-temperature end of the water droplet.[44] The viscous flows inside and outside the water droplets balance the Marangoni stress and drive the drop away from the laser as shown in Figure 1a. In the present geometry, the water droplet rests on a polystyrene Petri dish and is surrounded by decanol, resulting in a contact angle close to 180°. Thus, the contact area is small (the radius of the contact area is much smaller than the height of the drop) and the associated contact angle hysteresis restraining the droplet motion[45] is also small. This is a favorable situation, for it allows the adhesion of the drop to the surface without unduly restraining its motion driven by the laser. In the absence of this adhesion, the drops could easily escape due to convective fluid flow, instrument vibrations, and Brownian motion. This droplet geometry is different from theoretical work on thermocapillary migration that reports the analysis of liquid drop motion on horizontal surfaces for which the liquid drop height is significantly smaller than the radius of the drop contact area.[46, 47]

In this report, we show that water droplets covered by a surfactant or lipid monolayer immersed in an organic liquid (decanol or mineral oil) can be controlled using infrared light via the both thermocapillary effect and convection. These droplets sink to the bottom of the Petri dish ($\rho_{decanol}$ = 0.829 g/mL at 25 °C, $\rho_{mineral\ oil}$ = 0.82-0.88 g/mL at 25 °C, www.sigmaaldrich.com) and can be manipulated using optical forces. The experimental schematic is shown in Figure 1b. As shown in the figure, the water droplets are completely immersed in the organic phase. The incident laser is shown to exit at the organic-air interface. In this geometry, several forces are at play. When the laser is incident at the water-organic interface, a temperature dependent change in the interfacial tension can give rise to the thermal Marangoni effect as described in the preceding paragraph. The water droplet interface is dragged in the direction of increasing surface tension. In the presence of surfactant molecules at this interface a second effect called the solutal Marangoni effect sets in.[44] Here, the surfactants at the interface are dragged along the interface towards the high interfacial tension region. Thus, the diffusing surfactants tend to increase in concentration at the droplet edge where the interfacial tension increases. This surfactant buildup often negates the initial increase in interfacial tension. The two effects act against each other and often tend to arrest the drop

mobility.48-51 In spite of this, it is still possible to move droplets with interfacial amphiphiles when the solubility of the amphiphile is sufficiently high, in which case transport of the amphiphile through the bulk water or organic phase can counter the amphiphile gradients produced by the solutal Marangoni force, restoring a net force to move droplets. The heating from the laser radiation can also create forces on the droplets through convective fluid motion. Convection can be produced either through buoyancy due to the drop in density of the organic phase with increasing temperature (called natural convection) or surface tension gradients at the organic phase / air interface, which produces fluid flows in a manner similar to the thermal Marangoni droplet motion (called thermocapillary or Marangoni convection). Thermocapillary convection dominates over natural convection when the thickness of the organic phase is sufficiently small.[52] A number of observations support the presence of thermal Marangoni and convective droplet transport in our experiments. For example, for droplet motion ascribed to thermal Marangoni transport we observe repulsion of target droplets by the laser beam, interior circulation in droplets (see Figure 4 below), and loss of this motion when switching from a short to long lipid. Furthermore, thermal Marangoni based droplet motion is characterized by lower laser powers but higher thermal gradients (i.e., the laser beam must intersect the droplet). All observations support the presence of thermal Marangoni droplet transport. For motion ascribed to convection we observe movement of droplets toward the laser beam, movement of droplets even a distances of 100's of microns from the laser focus, droplets that sometimes pop off the surface and are transported toward the top of the organic phase, motion of non-deformable particles (polystyrene microspheres) that follow the same behavior as the deformable droplets, and a requirement for higher laser powers, and the laser does not need to intersect the droplet. Although these two effects describe our experiments quite well, it is entirely possible that other mechanisms such as the Soret effect or thermal diffusion effect[53] could play a role under certain circumstances.

The thermal Marangoni effect is found to persist in the decanol-water system in the presence of surfactants soluble in the water phase. Water droplets with a surfactant monolayer at the water-decanol interface can be brought into contact to form adhesive droplet pairs. These surfactant bilayers are either metastable or proceed into rapid coalescence if the resulting bilayer is unstable. We also show that metastable adhesive droplet pairs with short lipids can be utilized for controlled mixing of aqueous drops at a determined time through optically-driven surfactant bilayer rupture. This technique also provides a means to study interfacial film drainage and dynamics in such emulsions. In the case of longer lipids that are insoluble in water, droplet motion was only possible when laser heating set up convection currents in the external organic phase. The resulting lipid bilayers at the interface of two adhering aqueous droplets are stable over several hours.

Materials and Methods

Sodium dodecyl sulfate (SDS), decanol, and mineral oil were purchased from Sigma. A short chain lipid, 1,2-didecanoyl-*sn*-glycero-3-[phospho-*rac*-(1-glycerol)] (sodium salt) (10:0 PG) and a synthetic lipid, 1,2-diphytanoyl-*sn*-glycero-3-phosphocholine (4ME 16:0 PC, DphPC) were purchased from Avanti Polar Lipids Inc and were received dissolved in chloroform. Deionized water (DI) or phosphate buffered saline (PBS, Sigma) were used for all experiments to make aqueous lipid solutions. The optical set up included a 1457 nm infrared (IR) diode laser (FOL 1402PLY-617-1457, Furukawa Electric) and a co-aligned 660 nm red diode laser to assist the alignment of the IR beam into the microscope. An inverted Nikon Diaphot TMD or a Nikon TE-2000 was used for the microscope platform.[10] Two lenses in a 4f arrangement were used to facilitate alignment and focus the laser at the microscope image plane for experiments performed on the Diaphot TMD. The laser power measured at the 10× microscope objective used for observations on the Nikon Diaphot TMD microscope could be varied between 0-15 mW for experiments with the short chain lipid. Data with aqueous SDS droplets

were obtained without recording the laser power at the 10× objective; however the total laser power was estimated to be below 15 mW at the objective. Objectives used on the Nikon TE-2000 included 4× and 10× magnifications. The maximum laser power measured at the 4× objective on this microscope was 15 mW for the present experiments. The laser was steered into the microscope objective via direct reflection off the dichroic mirror in the filter cube. For experiments performed on the diaphot TMD, the focus position of the IR laser was determined using a phosphor powder film in a Petri dish. The phosphor powder glowed intensely when the laser was in focus. The spot size of the IR laser beam was approximately 100 μm^2.

For experiments using SDS and the short chain lipid 10:0 PG, decanol was used as the organic phase and was saturated with deionized water (DI) prior to use. Experiments with DphPC were performed using mineral oil as the organic phase. Lipid aqueous solutions were prepared by evaporating chloroform from a calculated volume of the lipid stock solution. Chloroform is a recognized carcinogen and the evaporation step was performed in a fume hood. The sample was also placed in a vacuum oven for 2 hours to remove residual chloroform in some instances when the film did not appear completely dry. The resulting lipid film was hydrated with DI water (10:0 PG) or PBS buffer (for DphPC) to yield the desired target lipid concentration. Lipid concentrations in the aqueous solutions were calculated to yield at least a monolayer of lipid coverage at the water-organic interface for the drops. Short chain lipids and SDS have sufficient solubility in water to reach this concentration given their high critical micelle concentration (CMC) values. These molecules self assemble in water to form micelles at concentrations above their CMC. For DphPC, there is insufficient solubility in water and these lipid molecules were introduced into aqueous droplets as vesicles. Lipid vesicles were formed via the extrusion technique in which the hydrated lipid solution was extruded through a 0.1 μm polycarbonate film in a mini-extruder (Avanti Polar Lipids) to yield a 1 mg/ml lipid solution in PBS. Aqueous drops in the organic phase were prepared by drawing a 34 gauge syringe needle (Microfil, WPI) containing the lipid solution through two to three ml of decanol or mineral oil placed in a Petri dish. The average radius of the drops was approximately 150 microns for drops in decanol and about 400 microns for drops in mineral oil. A 50% decrease in transmission of the 1457 nm laser beam through decanol was noted in our experiments. This observation is in agreement with the published spectra of the neat liquid.[54]

Results and Discussion

Previous work from our lab has established the use of optical radiation to move water drops immersed in decanol via the thermocapillary effect.10 As discussed in the Introduction, the presence of surfactants is expected to counter the droplet migration49, [50] through the solutal Marangoni effect. We demonstrate the persistence of droplet mobility in this system upon surfactant addition. We have observed varied behavior from water drops containing anionic surfactants such as SDS and the short chain lipid 10:0 PG on laser heating when immersed in decanol. SDS has a high critical micelle concentration (CMC) of approximately 8.2 mM[55] while the short chain lipid has a CMC of 0.42 mM.56 Both dissolve easily in water. For a drop of radius 150 microns, the concentration of SDS or the short chain lipid in the aqueous phase required for the formation of a uniform monolayer at the decanol-water interface is 0.05 mM (the lipid head group area is 66 $Å^2$ 56; the SDS head group area is comparable55). In the present work, the concentration of SDS was varied between 0.08 mM and 0.34 mM while the concentration of 10:0 PG in the aqueous solution was fixed at 0.8 mM, well above the CMC for this lipid. The latter ensured that the water-decanol interface was always covered with a lipid monolayer. Any excess lipid molecules will remain in the water phase as micelles and monomers in dynamic equilibrium.

Droplets containing SDS molecules

Droplet motion induced by the thermocapillary effect on laser heating was a common observation for these water droplets. For droplets containing SDS molecules, droplet coalescence was often observed, but the route followed by different pairs to the coalesced state varied. For example, for a set of observations in which the SDS concentration in the droplets was 0.08 mM, two SDS coated aqueous drops were brought into proximity over a distance of about 40 microns. The target drop (i.e., the one being moved by the laser) moved rapidly and interacted with the proximal (neighboring) drop over approximately 3 camera frames after which, the drops coalesced. It appeared that the droplets coalesced via the formation of an interface that had limited stability (Figure 2). It is important to note that the concentration of SDS was close to that required for monolayer coverage and it is possible that the larger drop had incomplete coverage. In a second set of observations, shown in Figure 3, the IR laser was positioned at the edge of a target droplet that was close to a neighboring droplet (the droplets were “almost” touching each other as viewed by the camera). When the laser was turned on, the target drop was observed to be pushed into the proximal droplet. During the droplet pair interaction, a dimple was observed (Figure 3c) preceding the formation of a wave-like feature that spread outward towards the edge of the interacting, almost flat interface. Eventually a surfactant bilayer film (Figure 3f) was formed that was not stable, rupturing in the consecutive frame and resulting in the coalescence of the droplets. The SDS concentration was 0.34 mM for this set of observations. The laser was incident on the target drop until the interface was formed.

These observations can be explained by providing a brief review of the forces that govern droplet pair interactions in emulsions. Two types of forces govern these interactions: One type is related to the surface forces that arise from intermolecular interactions (van der Waals, electrostatic, and steric or entropic interactions). These result in the presence of a disjoining pressure between interacting droplet pairs. The second type of force arises from the hydrodynamic flows around approaching droplets and the flow of the interfacial continuous phase, which slows the adhesion of the two surfactant layers. Once the droplets begin to interact under the combination of these two types of forces, their interaction can follow several paths. The possibilities, pictorially summarized by Danov *et al.*,57 provide a fundamental basis for exploring interfacial film formation in emulsions. The final stage in the evolution of the thin liquid film during droplet interaction is the formation of a “Newton black film” (NBF) and consists of a surfactant bilayer. This bilayer may remain stable on the order of minutes, or it may rupture rapidly after formation, resulting in the coalescence of the two droplets. Several mechanisms could give rise to the rupture of such metastable NBFs. Two routes are often cited in reviews[58]: (1) a mechanical instability and (2) thermally-activated pore formation. Mechanical instability is due to thermal capillary fluctuations in the film. One capillary mode (peristaltic) can become unstable and result in the contact of the two opposite surfaces of the interacting droplets, leading to the breaking of the film followed by droplet coalescence. For the second rupture mechanism, a thermally activated pore forms in the bilayer film that grows once it reaches a critical size resulting in the coalescence of the droplets. In Figure 2 there is rapid droplet coalescence without the formation of a stable flat interface. It is possible that when the droplets interact, there is insufficient surfactant coverage at the drop interfaces (0.08 mM SDS concentration) which results in coalescence. For the data shown in Figure 3, the situation is different, showing formation of a flat interface that subsequently ruptures. The droplets contain more surfactant than those in Figure 2, thereby ensuring complete interface coverage prior to drop interaction. When the laser is turned on, the target droplet is observed to push into the proximal droplet and a consequent “dimple” (Figure 3c) is observed which then spreads out to the film boundary. The steps leading to the formation of the SDS bilayer follow the exact sequence mentioned in the review by Danov *et al.*,[57] where in the dimple is followed by the formation of a flat interface and then a NBF.

Droplets containing the short chain lipid, 10:0 PG

Experiments were also performed with short chain lipids that have a relatively high CMC value in water (the 10 carbon chain lipid 10:0 PG, see the Experimental Details section above). Aqueous droplets containing 0.8 mM of this lipid (a concentration greater than the CMC) were manipulated in decanol with the IR laser. These droplets had a lower mobility compared to the droplets containing SDS molecules and in some cases it was very difficult to move these droplets. Even with the limited droplet mobility, droplet adhesion was observed (Figure 4), but no dimple formation was noted. The adhesive interface consisting of a lipid bilayer remained robust for up to 30 min (the total observation time). In this system, the interface bilayer formation process consisted of three distinct steps: (1) the initial deformation of the droplet surfaces on contact, (2) the flattening of the interface, which resulted in a thin film of the decanol trapped between the two droplets and (3) the consequent draining of the decanol trapped between the interacting monolayers in sequential steps (supplementary online video), accompanied by an increase in the area of the adhesive interface which entered a final metastable state of a lipid bilayer. The increase in the adhesive film diameter was approximately 10 microns (for the data shown in Figure 4) as measured from the optical images with a corresponding area increase of almost 2500 μm^2 over three images, and approximately over 4 s. This data set also provided information on the flow fields produced in the droplets due to the thermocapillary motion. Specifically, an interior particle (possibly an air bubble) in the target droplet permitted visualization of the water flow field in response to the heating from the laser (Figure 4e, video in supplementary information). The particle is drawn towards the laser focus along the interface and then moves away from the laser into the interior of the droplet. This suggests that an internal fluid flow is set up along the interface as a reaction to the interface being pulled towards the laser. Another important observation from this data set points to mobility of the proximal drops towards the laser in response to increasing laser power. The motion of proximal droplets toward the target drop could result from either counter fluid flows set up by the thermocapillary motion of the target drop or laser-induced convection flows in the decanol phase. Because the smaller size of the thermocapillary-driven counter flows, they can only be significant quite close to the target drop, while the convection-driven flows are much larger and can move droplets much further away from the target drop. Following Figure 4b, when the droplets almost touch, the drops remain in contact as the laser power is reduced to zero. The increasing influence of viscosity during film drainage impedes closing the final gap between the droplets.[59] Instead of increasing the laser power at this position to assist in droplet adhesion, the laser was repositioned towards the center of the droplet to avoid excessive heating at the droplet-decanol interface (supplementary video) by moving the microscope stage. The droplets adhered almost immediately upon increasing the laser power and reached a stable bilayer after drainage of the decanol film.

From these observations we can conclude that the increasing interfacial tension at the decanol-water interface drags this interface in the direction of the laser and sets up flow fields inside the water droplet that are directed towards the laser focus along the interface and away from the laser in the central part of the droplet. These flows drive the motion of the droplet away from the laser. The solutal Marangoni effect, in which the surfactant molecules are also dragged along the interface, can contribute to droplet retardation. It is possible to remobilize droplets with the thermocapillary effect using high concentrations of surfactants.[51] In the case of soluble surfactants such as SDS and the short chain lipid used in this work, excess surfactant molecules present in the droplet phase as monomers and micelles will migrate to the water-decanol interface that is depleted of surfactants in response to the solutal Marangoni effect. The fluid flow set up in the drop in response to the change in the interfacial tension upon heating is expected to drive these micelles towards the droplet-decanol interface. These micelles will replenish any molecules lost due to the drag forces along the interface thereby enabling the drops to move via the thermal Marangoni effect.

An exciting observation in the present study was the ability to break adhesive interfaces like those formed in Figure 4. The same laser (1457 nm) was used to achieve interface rupture and consequent coalescence of the droplets. This is demonstrated in Figure 5 where the adhesive interface shown in Figure 4 was ruptured by positioning the IR laser at the center of the bilayer. As the laser power was increased, the adhesive energy of the droplets changed, causing the inter-droplet contact area to decrease and the droplets pulled away from each other. When the laser power was sufficiently high (here 6 mW), the bilayer ruptured and the droplets coalesced. As expected, the initial and final droplet diameters indicate that volume was conserved upon the fusion of the two drops. These results establish the novelty of this method as an alternative to circuit-based microfluidics to achieve controlled mixing between solutions. This method can also provide selective mixing of droplet contents at predetermined time points thereby paving the way for sequential chemical reactions or providing a selected mixing time for studying rapid kinetic reactions.

Formation of a lipid bilayer between droplet pairs was not always observed in our experiments. In several instances, the droplets coalesced even when the laser power was maintained at values well below the 8.5 mW used in the earlier example. We also observed some droplets to be “pinned” to surface of the Petri dish. In these cases, the droplets could not be set in motion at laser powers approaching 8 mW. However, in almost all the observations in the present study, proximal droplets that were not directly heated by the IR laser were observed to have limited to significant mobility towards the laser when the target droplet was heated and the laser power was increased. As mentioned above, in most cases this is due to convection rather than counter flows from thermocapillary migration.

Droplets containing the long chain lipid DphPC

Finally, we demonstrate that IR laser-based convective flows can be used to form physiologically relevant lipid bilayers between contacting aqueous drops as shown in Figure 6. The same 1457 nm IR laser can be used to optically steer aqueous drops containing lipid vesicles into proximity and consequent adhesion, resulting in a lipid bilayer film at the interface. In this study we have used DphPC, a synthetic lipid that has been used by various groups to form droplet based lipid bilayers.[60, 61] In our approach, like that of Hwang et al,[62] lipid molecules were introduced in the aqueous phase as vesicles at a concentration of 1 mg/ml. Again, a syringe was used to immerse vesicle laden aqueous drops in oil. In these sets of experiments, decanol was replaced with mineral oil. Decanol is not the ideal choice for the external organic phase when droplet adhesion is intended to form physiologically relevant lipid bilayers at the pair interface. Mineral oil was used in these experiments instead because it is non-polar and will not preferentially align at the organic-water interface like the decanol molecules. Further, mineral oil has been used in previous studies to form water-in-oil emulsions using lipid molecules.[63] The lipid laden droplets were large, of the order of 400 microns in diameter in our study. In this droplet system, we were unable to obtain any mobility induced via the thermocapillary effect. This is consistent with the insolubility of these lipids preventing countering of the solutal Marangoni effect through bulk-phase migration of the lipid. Hence, convective flows set up in the mineral oil due to laser absorption were used to manipulate the drops. Mineral oil has a comparable thermal conductivity to decanol.[14] When the IR laser was positioned to focus in the mineral oil at the center of a collection of 4 drops, convective flow was observed to mobilize the drops towards the laser. In this experiment, two of the four drops were found to be adherent at the start of the manipulation. We have occasionally observed such drop pairs in our study, which form during the process of making the drops with the fine gauge needle. By positioning the laser to steer the drops via convective heating, three additional lipid bilayers were formed between the drops sequentially (Figure 6).[64] These bilayer interfaces have been observed to be stable for up to several hours. Unlike the bilayer with the short lipid, these bilayers do not readily rupture with low laser powers. With the long lipid, we have shown

that droplet bilayer networks similar to those reported by Holden *et al*[61] can be formed using an all optical platform without the use of micromanipulators.

In summary we have established the capability of using the thermocapillary effect and convection to initiate amphiphile-coated droplet mobility in water-in-organic liquid emulsions housed in a Petri dish. The apparatus required is relatively simple, being limited to an inverted microscope and diode laser. The methods demonstrated in this report can be used to develop an optical platform to form lipid bilayers using emulsions with the lipid molecules dispersed as vesicles in the water phase. This system can also be used to study interfacial film dynamics in adhesive emulsions. The flexibility offered by the use of single laser to manipulate drops into contact via adhesion and the subsequent coalescence of these drop pairs paves the way for developing Petri dish based microfluidic systems that would allow a user the ability to mix drop contents on demand at specific times and build drop networks to study sequential biochemical reactions.

Supplementary Material

Refer to Web version on PubMed Central for supplementary material.

Acknowledgments

Funding via internal research and development funds from SRI International and from the NIH (grant number R21CA133537) are gratefully acknowledged. A. Vasilyev and A. Eid were supported by the NSF through the Research Experiences for Undergraduates Program.

References

1. Whitesides GM. The origins and the future of microfluidics. Nature 2006;442(7101):368–73. [PubMed: 16871203]
2. Farinas J, Chow AW, Wada HG. A microfluidic device for measuring cellular membrane potential. Anal Biochem 2001;295(2):138–42. [PubMed: 11488614]
3. Matsunaga T, Hosokawa M, Arakaki A, Taguchi T, Mori T, Tanaka T, Takeyama H. High-efficiency single-cell entrapment and fluorescence in situ hybridization analysis using a poly(dimethylsiloxane) microfluidic device integrated with a black poly(ethylene terephthalate) micromesh. Anal Chem 2008;80(13):5139–45. Epub 2008 Jun 7. [PubMed: 18537270]
4. Wheeler AR, Throndset WR, Whelan RJ, Leach AM, Zare RN, Liao YH, Farrell K, Manger ID, Daridon A. Microfluidic device for single-cell analysis. Anal Chem 2003;75(14):3581–6. [PubMed: 14570213]
5. Xia F, Jin W, Yin X, Fang Z. Single-cell analysis by electrochemical detection with a microfluidic device. J Chromatogr A 2005;1063(1-2):227–33. [PubMed: 15700475]
6. Mao H, Cremer PS, Manson MD. A sensitive, versatile microfluidic assay for bacterial chemotaxis. Proc Natl Acad Sci U S A 2003;100(9):5449–54. Epub 2003 Apr 18. [PubMed: 12704234]
7. Griffiths AD, Tawfik DS. Miniaturising the laboratory in emulsion droplets. Trends Biotechnol 2006;24(9):395–402. Epub 2006 Jul 14. [PubMed: 16843558]
8. Huebner A, Bratton D, Whyte G, Yang M, Demello AJ, Abell C, Hollfelder F. Static microdroplet arrays: a microfluidic device for droplet trapping, incubation and release for enzymatic and cell-based assays. Lab Chip 2009;9(5):692–8. Epub 2008 Nov 27. [PubMed: 19224019]
9. Schmitz CH, Rowat AC, Koster S, Weitz DA. Dropspots: a picoliter array in a microfluidic device. Lab Chip 2009;9(1):44–9. Epub 2008 Oct 28. [PubMed: 19209334]
10. Kotz KT, Noble KA, Faris GW. Optical microfluidics. Applied Physics Letters 2004;85(13):2658–2660.
11. Lindsay S, Vazquez T, Egatz-Gomez A, Loyprasert S, Garcia AA, Wang J. Discrete microfluidics with electrochemical detection. Analyst 2007;132(5):412–6. Epub 2007 Mar 5. [PubMed: 17471386]
12. Kotz KT, Gu Y, Faris GW. Optically addressed droplet-based protein assay. Journal Of The American Chemical Society 2005;127(16):5736–5737. [PubMed: 15839641]

13. Beer NR, Wheeler EK, Lee-Houghton L, Watkins N, Nasarabadi S, Hebert N, Leung P, Arnold DW, Bailey CG, Colston BW. On-chip single-copy real-time reverse-transcription PCR in isolated picoliter droplets. Anal Chem 2008;80(6):1854–8. Epub 2008 Feb 16. [PubMed: 18278951]
14. Kim H, Dixit S, Green CJ, Faris GW. Nanodroplet real-time PCR system with laser assisted heating. Opt Express 2009;17(1):218–27. [PubMed: 19129891]
15. Kim H, Vishniakou S, Faris GW. Petri dish PCR: laser-heated reactions in nanoliter droplet arrays. Lab Chip 2009;9(9):1230–5. Epub 2009 Jan 19. [PubMed: 19370241]
16. Huebner A, Srisa-Art M, Holt D, Abell C, Hollfelder F, Demello AJ, Edel JB. Quantitative detection of protein expression in single cells using droplet microfluidics. Chemical Communications 2007; (12):1218–1220. [PubMed: 17356761]
17. Koster S, Angile FE, Duan H, Agresti JJ, Wintner A, Schmitz C, Rowat AC, Merten CA, Pisignano D, Griffiths AD, Weitz DA. Drop-based microfluidic devices for encapsulation of single cells. Lab Chip 2008;8(7):1110–5. Epub 2008 May 23. [PubMed: 18584086]
18. Teh SY, Lin R, Hung LH, Lee AP. Droplet microfluidics. Lab Chip 2008;8(2):198–220. Epub 2008 Jan 11. [PubMed: 18231657]
19. Sgro AE, Allen PB, Chiu DT. Thermoelectric manipulation of aqueous droplets in microfluidic devices. Anal Chem 2007;79(13):4845–51. Epub 2007 Jun 2. [PubMed: 17542555]
20. Daniel S, Chaudhury MK, de Gennes PG. Vibration-actuated drop motion on surfaces for batch microfluidic processes. Langmuir 2005;21(9):4240–8. [PubMed: 15836001]
21. Singh P, Aubry N. Transport and deformation of droplets in a microdevice using dielectrophoresis. Electrophoresis 2007;28(4):644–657. [PubMed: 17304498]
22. Egatz-Gomez A, Melle S, Garcia AA, Lindsay SA, Marquez M, Dominguez-Garcia P, Rubio MA, Picraux ST, Taraci JL, Clement T, Yang D, Hayes MA, Gust D. Discrete magnetic microfluidics. Applied Physics Letters 2006;89(3):034106.
23. Lee J, Moon H, Fowler J, Schoellhammer T, Kim CJ. Electrowetting and electrowetting-on-dielectric for microscale liquid handling. Sensors And Actuators A-Physical 2002;95(2-3):259–268.
24. Aarts DG, Lekkerkerker HN, Guo H, Wegdam GH, Bonn D. Hydrodynamics of droplet coalescence. Phys Rev Lett 2005;95(16):164503. Epub 2005 Oct 11. [PubMed: 16241805]
25. Bremond N, Thiam AR, Bibette J. Decompressing emulsion droplets favors coalescence. Physical Review Letters 2008;100(2):024501. [PubMed: 18232876]
26. Funfschilling D, Debas H, Li HZ, Mason TG. Flow-field dynamics during droplet formation by dripping in hydrodynamic-focusing microfluidics. Physical Review E 2009;80(1):015301.
27. Salmon JB, Leng J. Microfluidics for kinetic inspection of phase diagrams. Comptes Rendus Chimie 2009;12(1-2):258–269.
28. Verdier C, Brizard M. Understanding droplet coalescence and its use to estimate interfacial tension. Rheologica Acta 2002;41(6):514–523.
29. Baret JC, Kleinschmidt F, El Harrak A, Griffiths AD. Kinetic aspects of emulsion stabilization by surfactants: a microfluidic analysis. Langmuir 2009;25(11):6088–93. [PubMed: 19292501]
30. Thiam AR, Bremond N, Bibette J. Breaking of an emulsion under an ac electric field. Phys Rev Lett 2009;102(18):188304. Epub 2009 May 7. [PubMed: 19518918]
31. Baroud CN, Delville JP, Gallaire F, Wunenburger R. Thermocapillary valve for droplet production and sorting. Phys Rev E Stat Nonlin Soft Matter Phys 2007;75(4 Pt 2):046302. Epub 2007 Apr 5. [PubMed: 17500988]
32. Delville JP, de Saint Vincent MR, Schroll RD, Chraibi H, Issenmann B, Wunenburger R, Lasseux D, Zhang WW, Brasselet E. Laser microfluidics: fluid actuation by light. Journal Of Optics A-Pure And Applied Optics 2009;11(3):034015.
33. Nagy PT, Neitzel GP. Optical levitation and transport of microdroplets: Proof of concept. Physics Of Fluids 2008;20(10):101703.
34. Cordero ML, Burnham DR, Baroud CN, McGloin D. Thermocapillary manipulation of droplets using holographic beam shaping: Microfluidic pin ball. Applied Physics Letters 2008;93(3):034107.
35. Saint Vincent MRD, Wunenburger R, Delville JP. Laser switching and sorting for high speed digital microfluidics. Applied Physics Letters 2008;92(15):154105.

36. Hu H, Larson RG. Analysis of the effects of Marangoni stresses on the microflow in an evaporating sessile droplet. Langmuir 2005;21(9):3972–80. [PubMed: 15835963]
37. Grigoriev RO, Schatz MF, Sharma V. Chaotic mixing in microdroplets. Lab Chip 2006;6(10):1369–72. Epub 2006 Jul 31. [PubMed: 17102851]
38. Cordero ML, Rolfsnes HO, Burnham DR, Campbell PA, McGloin D, Baroud CN. Mixing via thermocapillary generation of flow patterns inside a microfluidic drop. New Journal Of Physics 2009;11:075033.
39. Verneuil E, Cordero ML, Gallaire F, Baroud CN. Laser-Induced Force on a Microfluidic Drop: Origin and Magnitude. Langmuir 2009;25(9):5127–5134. [PubMed: 19358521]
40. Young NO, Goldstein JS, Block JM. The motion of bubbles in a vertical temperature gradient. Journal of Fluid Mechanics 1959;6:350–356.
41. Velarde MG. Drops, liquid layers and the Marangoni effect. Philosophical Transactions Of The Royal Society Of London Series A-Mathematical Physical And Engineering Sciences 1998;356(1739): 829–843.
42. Velarde MG, Rednikov AY, Ryazantsev YS. Drop motions and interfacial instability. Journal Of Physics-Condensed Matter 1996;8(47):9233–9247.
43. Villers D, Platten JK. Temperature-Dependence Of The Interfacial-Tension Between Water And Long-Chain Alcohols. Journal Of Physical Chemistry 1988;92(14):4023–4024.
44. Shankar Subramanian, R.; Balasubramaniam, R. The Motion of Bubbles and Drops in Reduced Gravity. Cambridge University Press; 2001.
45. Furmidge C. Studies at phase interfaces. I. The sliding of liquid drops on solid surfaces and a theory for spray retention. Journal of colloid science 1962;17(4):309–324.
46. Brochard F. Motions Of Droplets On Solid-Surfaces Induced By Chemical Or Thermal-Gradients. Langmuir 1989;5(2):432–438.
47. Pratap V, Moumen N, Subramanian RS. Thermocapillary motion of a liquid drop on a horizontal solid surface. Langmuir 2008;24(9):5185–93. Epub 2008 Apr 10. [PubMed: 18399689]
48. Chiang TH, Wu TC, Yang YM, Maa JR. Bulk liquid soluble surfactant induced retardation of the thermocapillary migration of a droplet. Journal Of The Chinese Institute Of Chemical Engineers 2000;31(2):167–175.
49. Chen JN, Stebe KJ. Surfactant-induced retardation of the thermocapillary migration of a droplet. Journal Of Fluid Mechanics 1997;340:35–59.
50. Stebe KJ, Lin SY, Maldarelli C. Remobilizing Surfactant Retarded Fluid Particle Interfaces.1. Stress-Free Conditions At The Interfaces Of Micellar Solutions Of Surfactants With Fast Sorption Kinetics. Physics Of Fluids A-Fluid Dynamics 1991;3(1):3–20.
51. Wang YP, Papageorgiou DT, Maldarelli C. Increased mobility of a surfactant-retarded bubble at high bulk concentrations. Journal Of Fluid Mechanics 1999;390:251–270.
52. Vela E, Hafez M, Regnier S. Laser-Induced Thermocapillary Convection For Mesoscale Manipulation. International Journal Of Optomechatronics 2009;3(4):289–302.
53. Vigolo D, Brambilla G, Piazza R. Thermophoresis of microemulsion droplets: size dependence of the Soret effect. Phys Rev E Stat Nonlin Soft Matter Phys 2007;75(4 Pt 1):040401. Epub 2007 Apr 2. [PubMed: 17500850]
54. Czarnecki MA, Ozaki Y. The temperature-induced changes in hydrogen bonding of decan-1-ol in the pure liquid phase studied by two-dimensional Fourier transform near-infrared correlation spectroscopy. Physical Chemistry Chemical Physics 1999;1(5):797–800.
55. Butt, HJ.; Graf, K.; Kappl, M. Physics and Chemistry of Interfaces. Wiley-VCH; 2003.
56. Kleinschmidt JH, Tamm LK. Structural transitions in short-chain lipid assemblies studied by P-31-NMR spectroscopy. Biophysical Journal 2002;83(2):994–1003. [PubMed: 12124281]
57. Danov, KD.; Kralchevsky, PA.; Ivanov, IB. Dynamic processes in surfactant stabilized emulsions. In: Sjöblom, J., editor. Encyclopedic Handbook of Emulsion Technology. CRC Press; 2001. p. 621-659.
58. Bibette J, Calderon FL, Poulin P. Emulsions: basic principles. Reports On Progress In Physics 1999;62 (6):969–1033.

59. Chesters AK, Bazhlekov IB. Effect of insoluble surfactants on drainage and rupture of a film between drops interacting under a constant force. Journal Of Colloid And Interface Science 2000;230(2):229–243. [PubMed: 11017729]

60. Funakoshi K, Suzuki H, Takeuchi S. Lipid bilayer formation by contacting monolayers in a microfluidic device for membrane protein analysis. Analytical Chemistry 2006;78(24):8169–8174. [PubMed: 17165804]

61. Holden MA, Needham D, Bayley H. Functional bionetworks from nanoliter water droplets. J Am Chem Soc 2007;129(27):8650–5. Epub 2007 Jun 16. [PubMed: 17571891]

62. Hwang WL, Chen M, Cronin B, Holden MA, Bayley H. Asymmetric droplet interface bilayers. J Am Chem Soc 2008;130(18):5878–9. [PubMed: 18407631]

63. Hase M, Yamada A, Hamada T, Baigl D, Yoshikawa K. Manipulation of cell-sized phospholipid-coated microdroplets and their use as biochemical microreactors. Langmuir 2007;23(2):348–352. [PubMed: 17209573]

64. Poulin P, Bibette J. Adhesion of water droplets in organic solvent. Langmuir 1998;14(22):6341–6343.

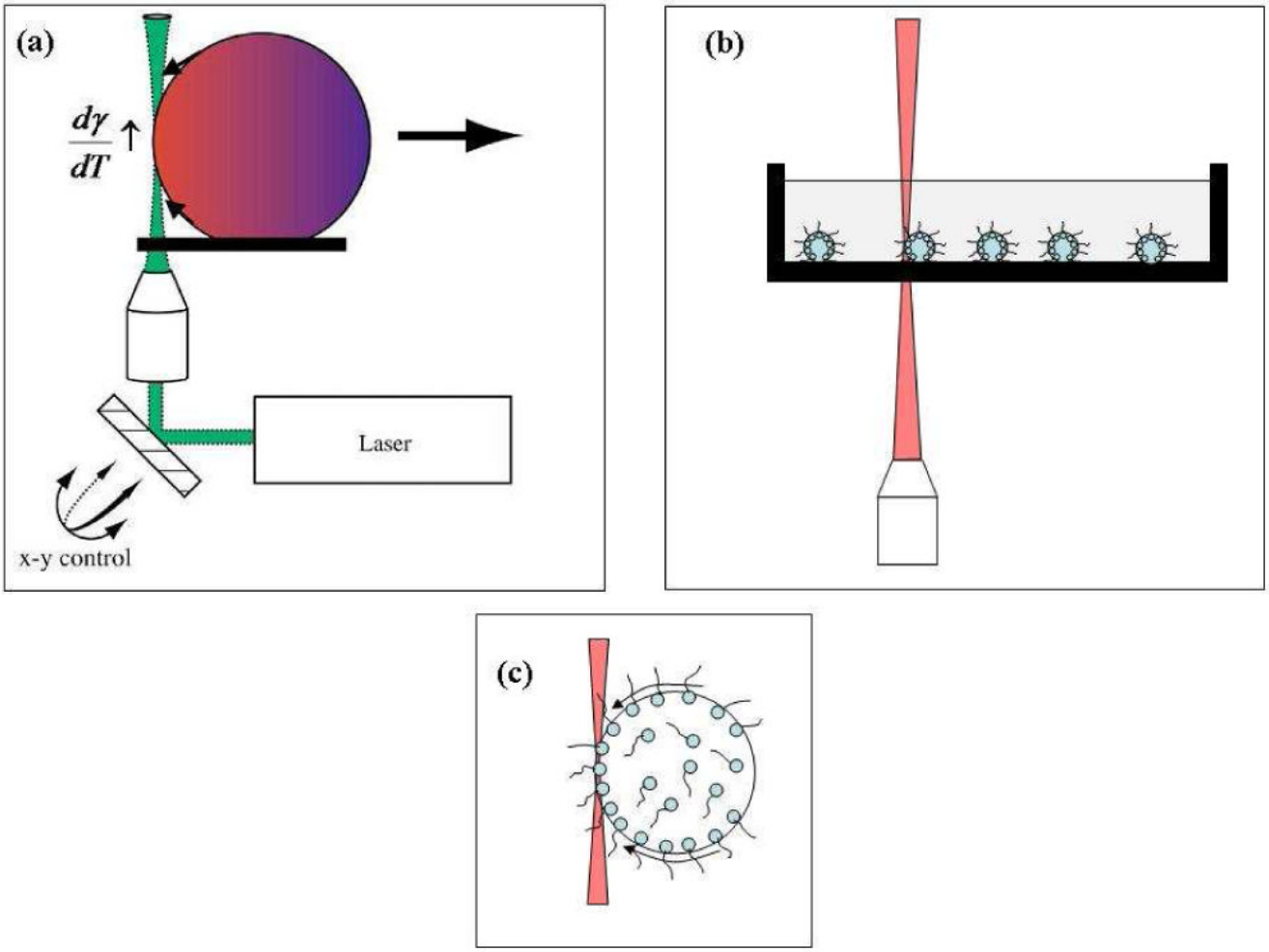

Figure 1.

(a) Schematic demonstrating the basis of thermocapillary motion in the water-decanol system. The arrows along the drop curvature indicate the direction in which the interface is pulled. The drop is propelled away from the laser. Adapted from Kotz *et al.*[10] (b) The experimental system shown here to emphasize the presence of surfactants and the complete immersion of the droplets. (c) A schematic of the solutal Marangoni effect. The black arrows point to the direction in which the interface is pulled. The surfactant molecules are dragged along the interface and accumulate at the droplet end with high surface tension, reducing the surface tension difference.

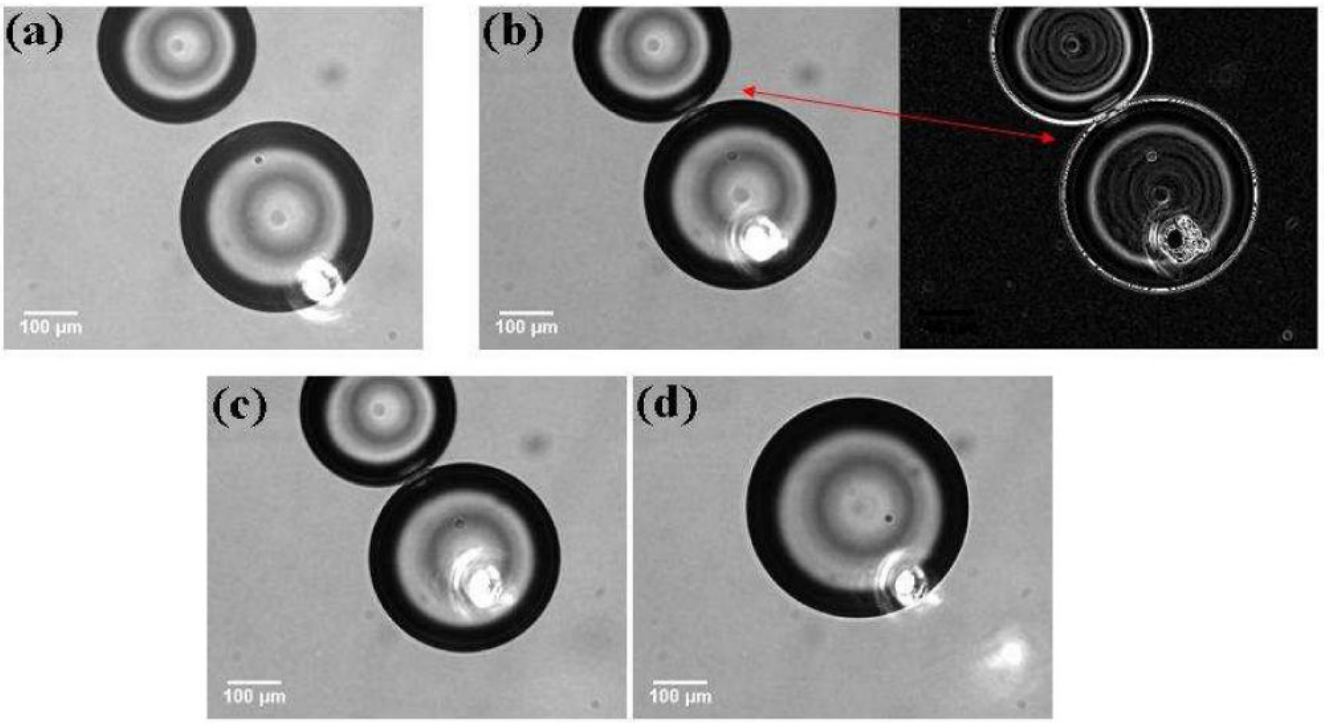

Figure 2.
Coalescence of SDS-coated water drops in decanol induced by the thermocapillary migration of the target drop. The SDS concentration was 0.08 mM. An interaction zone is observed in 2 (b) and 2(c). The inverse image in (b) was processed using ImageJ software (NIH) to enhance drop edges. The position of the IR laser is marked by the bright spot from the visible red laser in each image.

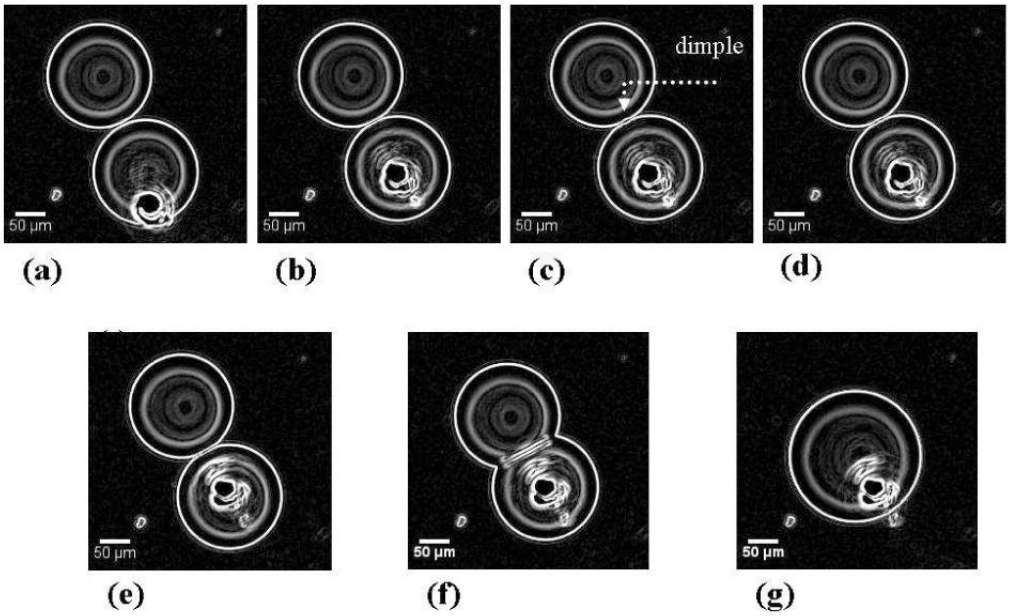

Figure 3.

Steps observed during the interaction of SDS coated water droplets in decanol. The SDS concentration was 0.34 mM. The images obtained from the camera were processed using ImageJ software (NIH) to enhance the drop edges. The position of the red laser is marked by the “white” blob at the base of the target drop. The dimple is observed to form when the laser power is increased and the target drop is pushed into the proximal drop.

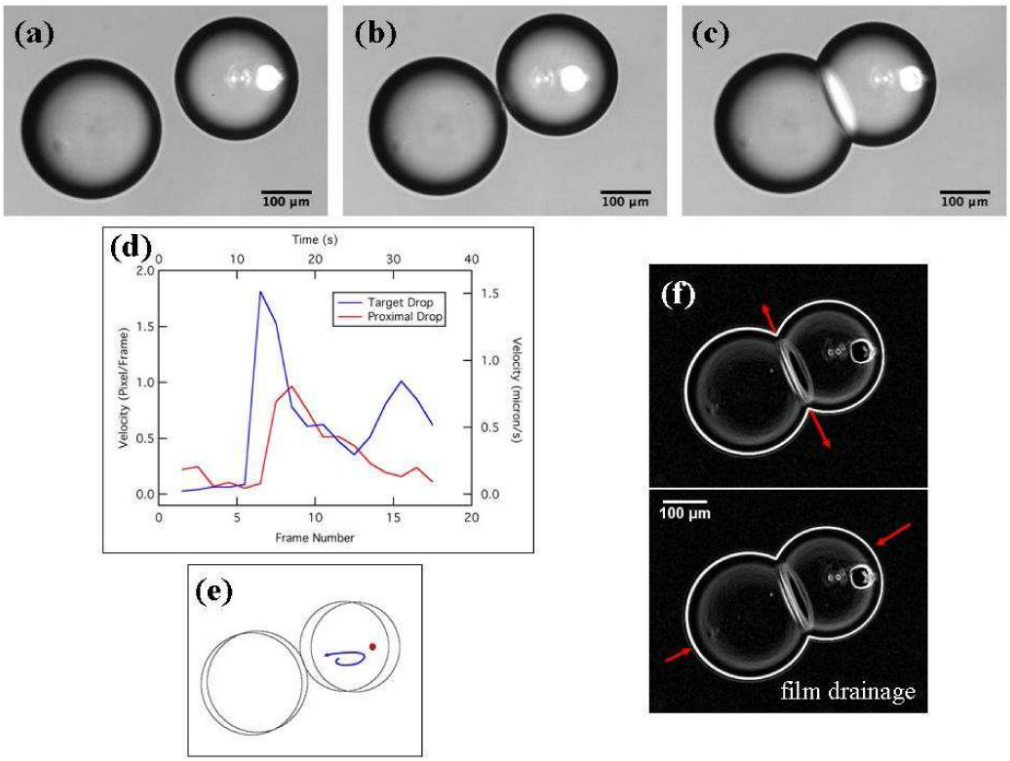

Figure 4.

IR-laser-induced motion of a target water drop containing 10:0 PG at 0.8 mM. (a, b) The target drop moves when the IR laser is switched on. The bright laser spot seen in the images is from the visible red laser used solely to guide the IR laser beam. Once the drops almost touched, the laser power was reduced to zero and the position of the stage was changed as shown in (b) to reposition the laser to be incident inside the target drop to assist in droplet adhesion. (c) Contact between the pair of aqueous drops and the consequent formation of the lipid bilayer; see the text for details. Note that although the laser position is stationary and the microscope stage was moved to change the position of the laser relative to the droplets, the images in (a)-(c) and the video have been cropped to show a stationary view relative to the microscope slide. By fixing the image reference frame to the microscope slide in this way, the images better elucidate the motion of the droplets relative to each other. (d) Plot of the speeds of the target and proximal drops as a function of the frame number or time. The target drop has a larger velocity and faster response when the laser power is turned on. The velocity is measured for frames leading to drop contact only. Each rise in the target drop velocity corresponds to a sequential increase in laser power. (e) Schematic depicting the path traced by a particle in the target water drop on laser heating of the water-decanol interface between frames (a) and (b). (f) Drainage of the decanol organic phase between interacting lipid monolayers of the droplet pair is denoted by the red arrows at the droplet pair interface. The increase in the interface area is denoted by the red arrows opposite the interface and indicates a flattening of each drop. The image is a processed version of the original data using ImageJ software. A video is available in the Supporting Information.

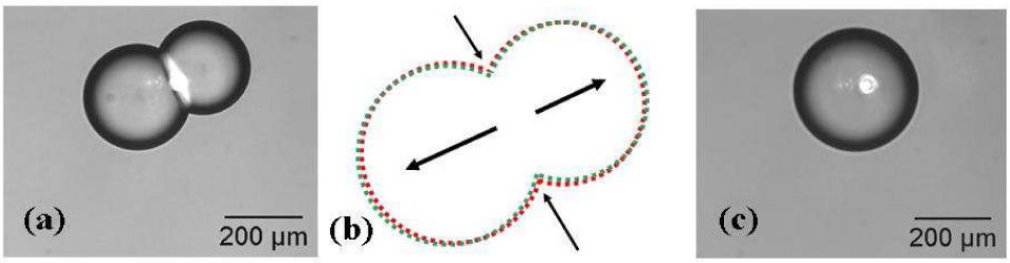

Figure 5.

The destruction of the lipid bilayer interface is followed by the coalescence of the droplet pair. (a) The laser is positioned on one side of the bilayer. (b) A schematic showing the sequence of events following laser heating of the interface. The two droplets retract from the interface thereby decreasing the interface area as denoted by the black arrows. (c) The droplets retract over three consecutive frames (i.e., over approximately 4 seconds) before the actual rupture of the bilayer that occurs in less than 2 seconds.

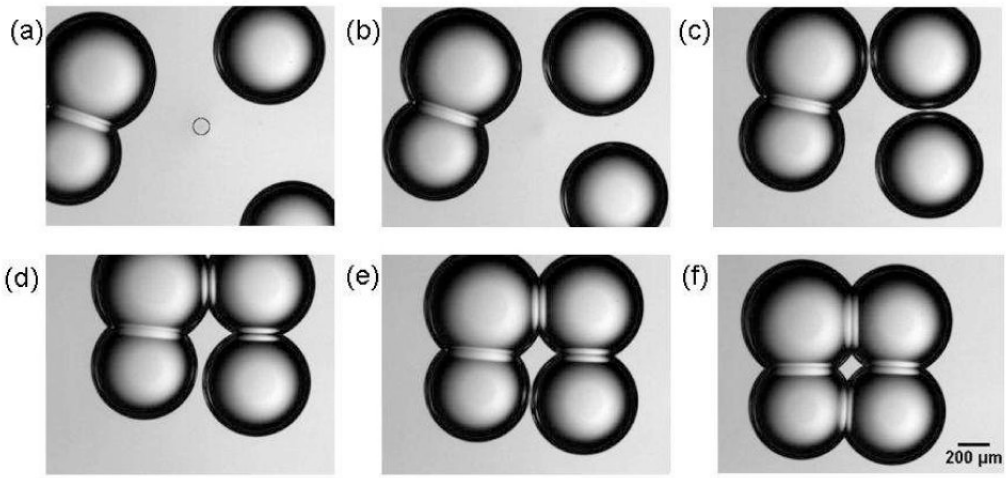

Figure 6.
Formation of a lipid bilayer interface using physiologically relevant lipids. The circle in frame (a) corresponds to the position of the IR laser. Convective heating drives the two non-adhering drops into proximity and adhesion results in the formation of four lipid bilayers. A supplementary video is available online.